Spring 5-2004

Concentration and sulfur isotopic composition of authigenic sulfide minerals at methane seep sites versus diffusive sites

V. Lynn Means
Eastern Kentucky University

Recommended Citation

Means, V. Lynn, "Concentration and sulfur isotopic composition of authigenic sulfide minerals at methane seep sites versus diffusive sites" (2004). *Geosciences Undergraduate Theses*. 1.
https://encompass.eku.edu/geo_undergradtheses/1

FINAL!

CONCENTRATION AND SULFUR ISOTOPIC COMPOSITION OF AUTHIGENIC SULFIDE MINERALS AT METHANE SEEP SITES VERSUS DIFFUSIVE SITES

V. Lynn Means

A Senior Thesis in Geology,
submitted to Dr. Walter S. Borowski
Department of Earth Sciences
Eastern Kentucky University
May 2004

ABSTRACT

This study investigates the amount of sulfide sulfur and its sulfur isotopic composition ($\delta^{34}S$) in seep site sediments of the Blake Ridge Diapir (BRD; offshore southeastern United Sates) and Monterey Bay (offshore California, United States). The geochemistry of these sediments is influenced by anaerobic methane oxidation (AMO). Our aim is to compare the sulfur geochemistry of seeps sites, where advective delivery of methane is an important process, to other localities where AMO is also an important biogeochemical process but where diffusion is the dominant mass transport mechanism. Sulfide sulfur of authigenic sulfide minerals was extracted from sediments using chromium reduction. We measured sulfide sulfur concentration via iodometric titration and in separate runs obtained sulfide precipitate for $\delta^{34}S$ analyses. Our concentration measurements are flawed and the $\delta^{34}S$ data are pending, so we used data from other studies for our comparisons.

Methane seep sediments of Monterey Bay seem to have significantly higher sulfide content than do those from the BRD, but diffusive and advective sites cannot be distinguished by sulfide sulfur content alone. Data from the literature show that the ^{34}S content of sulfide minerals from seep sites (modal $\delta^{34}S$, ~ -30‰ CDT) is intermediate between that of diffusive sediments unaffected by AMO (modal $\delta^{34}S$, ~ -35‰) and those affected by AMO (modal $\delta^{34}S$, ~ -20‰). However, sulfide sulfur from seep sites and advective sites cannot be distinguished isotopically. Some samples from diffusive sediments located near the present-day sulfate-methane interface show unique sulfide sulfur isotopic compositions with strong ^{34}S enrichment ($\delta^{34}S > 0$ ‰).

TABLE OF CONTENTS

LIST OF TABLES

LIST OF FIGURES

Figure Page

LIST OF ABBREVIATIONS

Anaerobic Methane Oxidation	AMO
Bottom Simulating Reflectors	BSR
Ocean Drilling Program	ODP
Oxidation of sedimentary organic matter	SOM
Sulfate-Methane Interface	SMI
Sulfate Reduction Zone	SRZ
Zinc Acetate	ZnAc

Introduction

Sulfate depletion via sulfate reduction is an important biogeochemical process that takes place in marine sediments. This thesis paper deals with a study of the concentration and isotopic composition of sulfur found in deep-ocean sediments located on the Blake Ridge Diapir (offshore North Carolina) and a portion of Monterey Canyon (offshore California). These sites are methane seeps where methane travels quickly through the sediments, either in gaseous phase or as dissolved methane entrained within the upward-moving pore waters, often via fractures in the sediments (Paull et al., 1995; Kohn et al., 1998). The Blake Ridge Diapir is the southernmost diapir in a series of about 20 structures rising from depth within sediments in water depths of 2170 m (Egeberg, 2000). Paull et al. (1995) and Ocean Drilling Program Leg 164 (Paull et al., 1996) collected samples from the diapir, which are used in this study. The Monterey Bay region cold seep sites were first discovered in the axial valley of the Monterey Submarine Canyon during dives using the research submersible ALVIN (Embley et al., 1990). Kohn et al. (1998) have investigated the sulfur geochemistry of Monterey Bay seeps.

Sulfate reduction is a diagenetic process in which microbes deplete sulfate from pore water (e.g., Berner, 1980). Sulfate reduction occurs under anoxic conditions usually with redox potential (Eh) below –100 mV (Jorgensen 1990). The net process involves the reduction of sulfur in sulfate to sulfide. Sulfate reduction is responsible for about half of the organic carbon oxidation in the sediment in various settings (Jorgensen, 1990). Sulfate reduction in marine sediments occurs via two different pathways. The oxidation of sedimentary organic matter (SOM),

$$2\,(CH_2O) + SO_4^{2-} \rightarrow 2\,HCO_3^- + H_2S \text{ (Equation 1)},$$

is mediated by sulfate reducers (*Bacteria*). Anaerobic methane oxidation (AMO),

$$CH_4 + SO_4^{2-} \rightarrow HCO_3^- + HS^- + H_2O \text{ (Equation 2)},$$

is carried out by a consortium of sulfate reducers and methanotrophs (*Archaea*) (e.g., Borowski et al., 2002; Orphan et al., 2001).

There are a number of primary controls on sulfate depletion in marine sediments: temperature, the deposition of organic matter in the sediments, and methane delivery. Temperature influences the rate of sulfate reduction by controlling the rate of chemical reactions. In marine sediments, microbes are generally most active at the temperature range of 0-40°C, with an optimum temperature around 30-35°C (Jorgensen, 1990). However, temperature ranges in deep-sea sediments are rather uniform because bottom waters are typically cold and pore waters warm up along a geothermal gradient with increasing depth into the sediment (Borowski, personal communication). Thus, organic matter and methane delivery are the two main controls upon sulfate reduction processes.

The amount of organic matter deposited in sediments is the predominant control of sulfate reduction via SOM (Equation 1) in marine systems (Berner, 1980). Both the sedimentation rate (organic matter delivery) and the quality of the organic matter, or its degradability, affect sulfate reduction rates (Berner, 1980). In regions where organic matter delivery is low, and/or where organic matter quality is low, the amount of methane in the system becomes increasingly important (Borowski, 1998).

In such systems, as the amount of methane increases the biogeochemical importance of AMO (Equation 2) also increases (Borowski et al., 1996, 1999). Sulfate profiles in the Blake Ridge region seem largely influenced by AMO rather than SOM

(Borowski et al., 1996, 1997, 1999, 2000a). The carbon isotopic composition of the dissolved CO_2 shows derivation from methane and that at least 35% of the sulfate is depleted through AMO (Borowski et al., 2000a). AMO also impacts sulfur geochemistry in terms of authigenic sulfide mineral concentration and sulfur isotopic composition in such settings.

Dissolved sulfide is released into pore waters during sulfate reduction. If iron is present within the system, hydrogen sulfide ($\Sigma HS = H_2S, HS^-, S^{2-}$) and iron will react to produce authigenic sulfide minerals (elemental sulfur, S°; iron monosulfide, ~FeS; pyrite, FeS_2) as a solid precipitant (Berner 1980). If the iron content of pore waters is low, hydrogen sulfide will be produced faster than it is being scavenged by iron so that it will build in concentration and diffuse away from the production site (Berner, 1980). In SOM, dissolved sulfide can be produced anywhere within the sulfate reduction zone. In AMO, sulfide is focused in the lowermost sulfate reduction zone at the sulfate-methane interface (Borowski et al., 2000b), where both methane and sulfate co-exist at relatively low concentration (Borowski, 1998).

In sediments of the Blake Ridge, larger amounts of sulfide minerals occur near or below the SMI (Fig. 1) (Thompson et al., 2004; Borowski et al., in prep.). This is consistent with focused AMO occurring at the SMI, with less significant sulfur mineralization occurring higher in the sulfate reduction zone.

Sulfate reduction involves the fractionation of sulfur isotopes (Chambers and Trudinger, 1978). The most abundant stable sulfur isotopes exist as ^{32}S and ^{34}S, accounting for 95.02% and 4.21% of sulfur, respectively (Kendall and Snyder, 1995). As

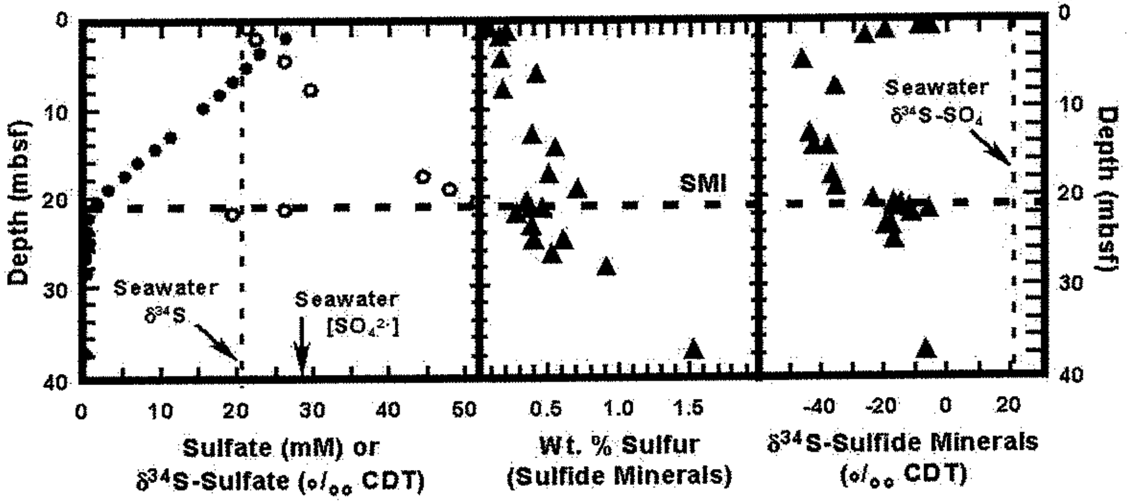

Figure 1. Typical sulfur geochemistry at a diffusive site of the Blake Ridge region. Shown are profiles of interstitial dissolved sulfate (SO_4^{2-}), sulfur isotopic composition of interstitial sulfate ($\delta^{34}S_{SO4}$) in per mil ($^{o}/_{oo}$) relative to the Canyon Diablo Troilite (CDT); sulfide sulfur content of sediments residing in bulk, authigenic sulfide minerals (collectively native sulfur, iron monosulfides, and pyrite) expressed in weight percent sulfur (Wt. %); and sulfur isotopic composition of sedimentary sulfide minerals ($\delta^{34}S_{\text{sulfide minerals}}$) at Ocean Drilling Program Site 995. The sulfur isotopic composition of modern seawater sulfate is shown by dashed vertical lines (Rees et al., 1978). Dashed horizontal lines indicate the sulfate-methane interface (SMI) as defined by interstitial sulfate and methane concentrations. Sulfate concentrations from the ODP sites are from Paull et al. (1996); other data are from Borowski et al. (2000b, in prep).

sulfate is depleted in the sediment, sulfate-reducing microbes preferentially use ^{32}S in both SOM and AMO, leaving pore water sulfate with higher amounts of ^{34}S. Thus, ^{34}S is usually found in higher abundance deeper in the sulfate reduction zone whereas ^{32}S is typically in higher abundance shallower in the sulfate reduction zone.

The type of methane transport will control methane delivery rate as diffusive mass transport is generally much slower than advective mass transport (Borowski, personal communication). At sites where methane diffuses through sediments, a zone is created where both methane and sulfate co-exist in pore water, the sulfate-methane interface (SMI). Here, active sulfide mineralization presumably occurs as AMO takes place (Borowski et al., submitted; Takacs & Borowski, 2003, 2004; Thompson et al., 2004). Modern sediments show enrichment in ^{34}S at the SMI relative to sulfide minerals located in the sulfate reduction zone (Fig. 1). Higher methane deliveries at advective locations cause the SMI to move closer to the seafloor, often to within centimeters of the sediment water interface (e.g., Paull et al. 1995). Tectonic activity at sites such as Blake Ridge and Monterey Canyon may create fractures in the sediment, which act as conduits for fluid flow causing a higher methane delivery rate. Increased methane delivery should increase the influence of AMO on the geochemistry of pore waters and sediments.

This paper will compare the concentration and sulfur isotopic composition of sulfide minerals produced at these two seep sites to that of sulfide minerals produced at non-seep sites where diffusive transport is predominant. The diffusive sites are located in the Blake Ridge region. We also use sulfur isotopic data from Kohn et al. (1996) from Monterey Bay seep sites for comparative purposes.

Methods

We extract sulfide sulfur from authigenic sulfide minerals within core samples taken from methane seep sites located at Blake Ridge Diapir (Fig. 2) and Monterey Canyon (Fig. 3). After a core is brought on board, a portion of it, ˜6-cm-thick is sampled and squeezed to extract pore waters. The dry squeeze-cake is sealed in a plastic bag for further study, ultimately freeze-dried, and is the source for sediments analyzed in this study.

Sediment samples are crushed using a mortar and pestle to a powder and stored in a glass vial. Each sample is put through two separate processes; one to determine the sulfide sulfur concentration and another to analyze the sulfur isotopic composition ($\delta^{34}S$) of the authigenic sulfide minerals.

Chromium reduction is used to extract sulfide sulfur (elemental sulfur, S^o; iron monosulfide, ~FeS; and pyrite, FeS_2) from sediment samples (Canfield et al., 1986). The chromium reduction procedure uses a distillation apparatus to extract sulfide sulfur. Nitrogen (N_2) is flushed into the extraction flask where sulfide sulfur is extracted from the sediment, producing hydrogen sulfide gas (H_2S). The H_2S is then carried by the N_2 through tubing into the trapping flask where either silver sulfide or zinc sulfide is precipitated.

The chromium reduction procedure consists of three steps. First mossy zinc is amalgamated. In amalgamation, approximately 500 g of mossy zinc is placed in a 1000-ml beaker. 75 ml of 2% mercuric chloride is added to the zinc. The beaker is then filled with 2N HCl to 1000 ml. Once bubbling has ceased (usually 20–30 minutes) the amalgamation process is complete. The liquid in the beaker is poured into a waste

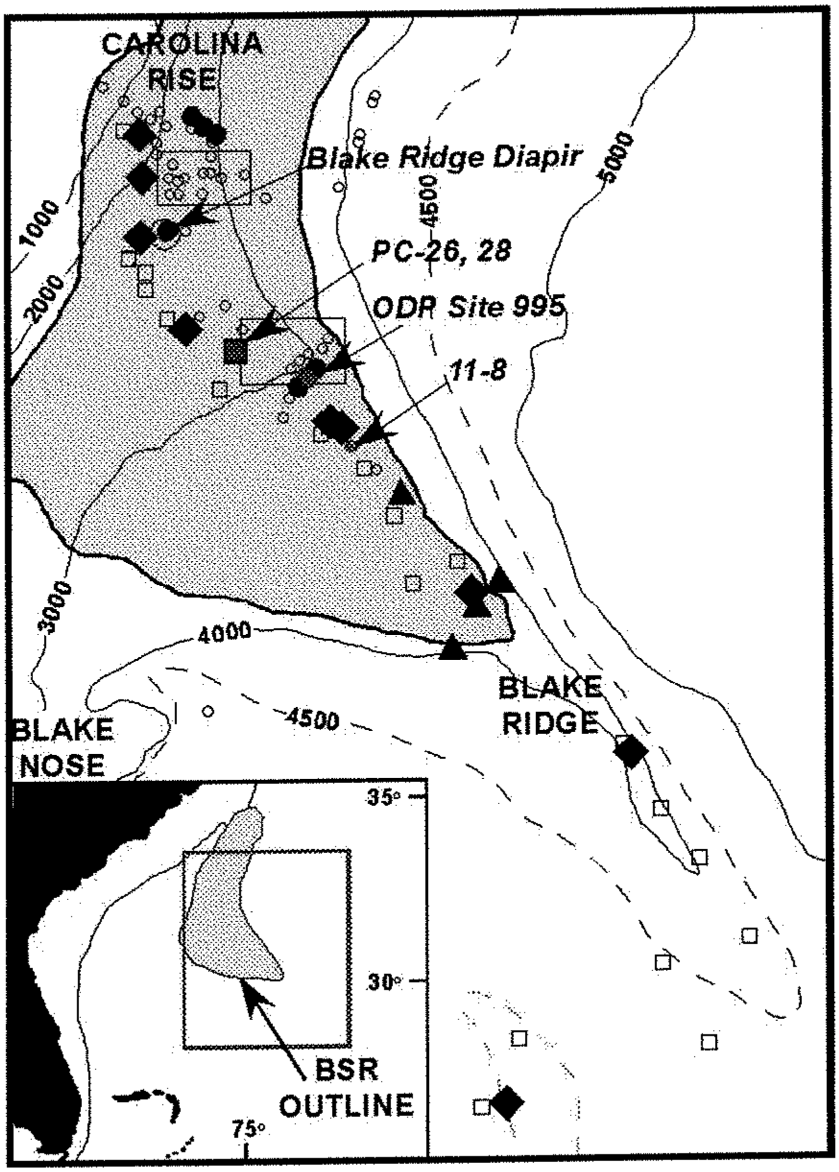

Figure 2. Location map for Blake Ridge region samples. This study analyzes samples taken at the methane seep sites (advective methane transport) of the Blake Ridge Diapir through both piston coring (cruise Kn-140-1-92, PC-2 and PC-3) and deep-sea drilling (Ocean Drilling Program, ODP Site 996). Other sample sites are dominated by diffusion rather than advection and include: piston core 11-8 (cruise CH-11-92, Borowski et al., in prep); ODP Site 995 (Takacs and Borowski, 2003, 2004); and piston cores 26 and 28 (cruise CH-15-2000, Thompson et al., 2004).

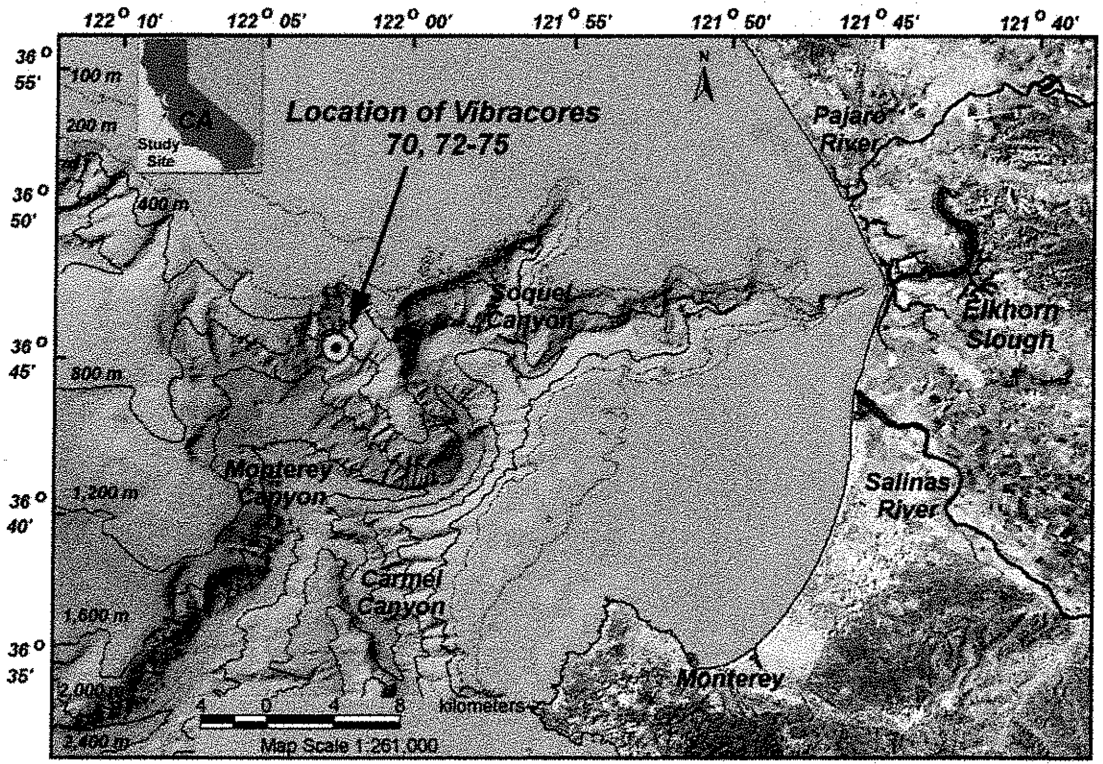

Figure 3. Location of vibracores at seep sites of Monterey Bay. Sites VC-70 and VC-73 are vibrocores taken with underwater remote guided vehicles (ROVs).

container. The zinc is then rinsed three times with double-distilled water and dried under a hood and is ready for use in the chromium reduction process.

Second, a chromic chloride solution is prepared by dissolving 266.5 g of chromic chloride hexahydrate ($CrCl_3 \cdot 6H_2O$) in 1000 ml of 2N HCl, producing a 1 M solution. Meanwhile approximately two finger widths of amalgamated zinc are placed in a plastic wash bottle and approximately 250 ml of chromic chloride is added. The wash bottle is sealed, connected to the nitrogen tank, and flushed with nitrogen creating an anoxic environment. Within 15–20 minutes the solution changes from dark green in color to bright blue in color, indicative of the valance change of $Cr^{+3} \rightarrow Cr^{+2}$. A short tube is attached to the wash bottle to maintain the anoxic environment while the solution is drawn into a 60 ml syringe. The zinc is rinsed three times with double-distilled water, dried, and can be re-amalgamated for future use.

A series of four flasks are operated simultaneously with flowing nitrogen gas (N_2) distributed through separate tubing connected to each flask (Canfield et al., 1986). Three samples and one pyrite standard are run at one time under a ventilated hood. The pyrite standard serves as a measure of extraction efficiency for each run; low sulfide-sulfur recoveries in the standard indicate a failed run that must be repeated. The sediment sample is placed into ground-glass reaction flask and moistened with 15 ml of 100% ethanol. The extraction apparatus is closed to the outside atmosphere in order to purge oxygen from the system with the N_2 carrier gas. Hot plate temperature is gradually raised to 250°C and cold water is flushed through the distillation apparatus via tubing. After preparation of the reduced chromic chloride solution, 60 ml of the solution is placed in each reaction flask along with 10 ml of 6N HCl via a ground-glass port. This is done as quickly as possible to maintain the anoxic environment. Addition of chromic chloride and acid stimulates dissolution of sulfide-sulfur minerals and the creation of hydrogen sulfide gas (H_2S), which is carried out of the reaction flask and into the trapping solution. Sulfide extraction should be complete after two hours of simmering; this time period is in excess of that suggested by Canfield et al. (1986).

A zinc acetate ($Zn(C_2H_3O_2) \cdot 2H_2O$) - ammonium hydroxide ($NH_4OH$) solution is used to precipitate sulfide sulfur via the chromium extraction technique for concentration measurements of sulfide sulfur. 60 g of zinc acetate is added to 100 ml of ammonium hydroxide (NH_4OH) and filled to 1000 ml with double distilled water to produce a 1 M solution. 60 ml of the solution (ZnAc + NH_4OH) is added to each 125-ml, Erlenmeyer trapping flask. After sulfide extraction, the trapping flask is removed and rinsed down with double-distilled water to ensure that all precipitant is contained within the solution.

The concentration of sulfide sulfur is measured through iodometric titration (Canfield et al., 1986), modified with a "back-titration" technique (Thompson and Borowski, 2003). The method involves the addition of 15 ml of a 0.1M solution of KIO_3/KI to the trapping solution. The KIO_3/KI solution is prepared by dissolving 0.535 g KIO_3 and 2.5 g KI in 100 ml double-distilled water. A magnetic stirrer is placed in the trapping flask along with 15 ml of ~0.1 M KIO_3/KI solution and 10 ml 6N HCl and is immediately sealed with a rubber stopper to prevent the loss of H_2S gas. The flask is placed on a magnetic stirrer for 15 minutes and the solution is dark orange/yellow in color as dissolved sulfide is quantitively absorbed by the solution. A solution of ~0.8 M thiosulfate ($S_2O_3^{-2}$) is then prepared by dissolving 4 g of sodium thiosulfate ($Na_2(S_2O_3^{-2})$) and 0.05 g of sodium carbonate ($NaCO_3$), in 200 ml of boiling, double-distilled water.

The solution is stored in a 250 ml amber bottle; due to microbial degradation the solution must be prepared anew each day. For titration, a 50 ml titration burette is filled with the thiosulfate solution. While stirring the contents in the trapping flask, the thiosulfate titrant solution is gradually added until a pale yellow color occurs. Then, 2 ml of starch indicator solution is added to the trapped precipitant to turn the solution dark blue in color. Titration continues until the contents turn white or clear in color, indicating that the entire KIO_3/KI-sulfide sulfur complex has been neutralized by thiosulfate (Thompson and Borowski, 2003).

Silver sulfide (Ag_2S) precipitate is used for determination of the sulfur isotopic composition of sulfide minerals and involves a separate trapping step. A 1 M solution of silver nitrate ($AgNO_3$) is prepared by dissolving 21.23 g of solid $AgNO_3$ in 200 ml of double-distilled water within a 200 ml volumetric flask. 60 ml of this trapping solution is placed within the trapping flask of the chromium extraction apparatus. Hydrogen sulfide gas carried into the solution and precipitates as silver sulfide.

The silver sulfide is filtered, dried, weighed, and stored in a glass vial. Between 0.6–0.85 g of precipitant is weighed on a microbalance and placed into a tin foil package along with 3.0–3.6 g of vanadium oxide (V_2O_5) and sent to Indiana University for mass spectrometry using the general method of Holt and Engelkemeir (1970).

Results

Laboratory Results

Concentration and isotopic measurements of sulfide sulfur are dependent upon complete extraction of sulfide sulfur from samples and near-complete recovery of both ZnS and Ag_2S precipitates in the trapping flask. Samples of crystalline pyrite (FeS_2), with presumed sulfur content of ~53%, are used as a standard. Recovery data (Fig. 4) show either low recovery or recovery higher than stoichiometrically possible. In contrast, Canfield et al. (1986) report sulfur recovery approaching 100%. Our low recoveries greatly lower the confidence we have in our sulfide concentration measurements, and perhaps the forthcoming isotopic results. Moreover, we mistakenly ran many extraction sets without a pyrite standard.

The measurements of the concentration of authigenic sulfide minerals likely show unreliable results. Sulfide-sulfur content is determined from both iodometric and gravimetric analyses in order to cross check sulfide-sulfur concentration values. Sulfide sulfur concentration values from gravimetric analyses typically track to within 5% of values from titration (Takacs and Borowski, 2004). Measurements via iodometric titration typically show 10-20 weight percent sulfide sulfur in the sediments - far greater than the content as determined by gravimetric determination of Ag_2S precipitant, which show 0.22–1.55 weight percent sulfide sulfur (Table 2, Fig. 5).

Because of widely variant concentration values from both methods and because of poor sulfur recoveries, we are unable to determine if either method yields correct results. Marine sediments typically contain 1–2% sulfide sulfur (e.g., Berner, 1980; Goldhaber

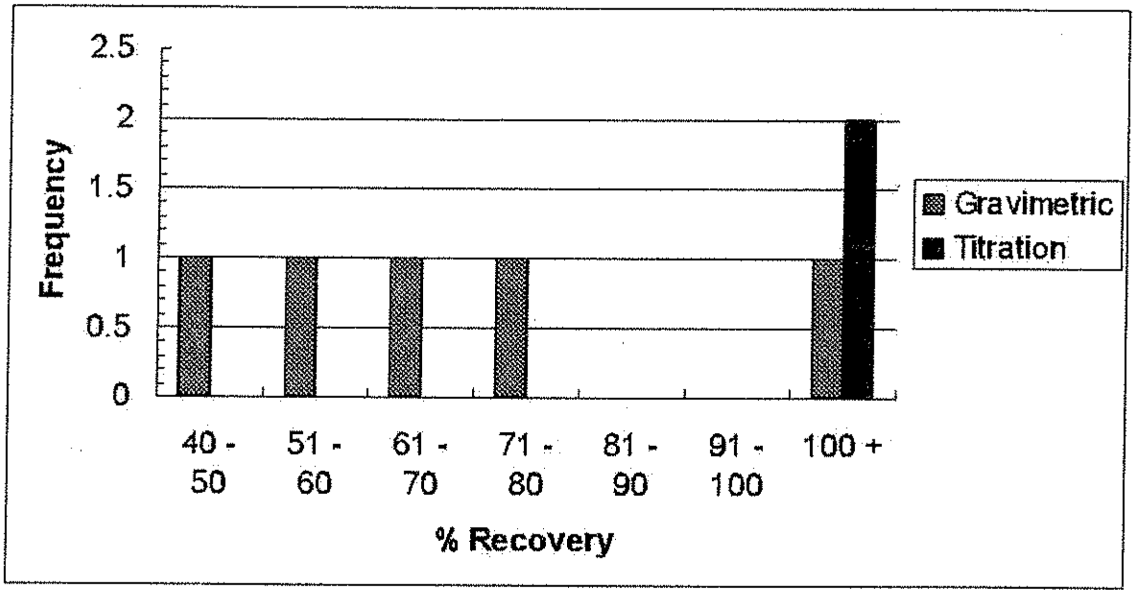

Figure 4. Recovery of sulfide sulfur from pyrite standards. Laboratory recovery rates in general were very poor.

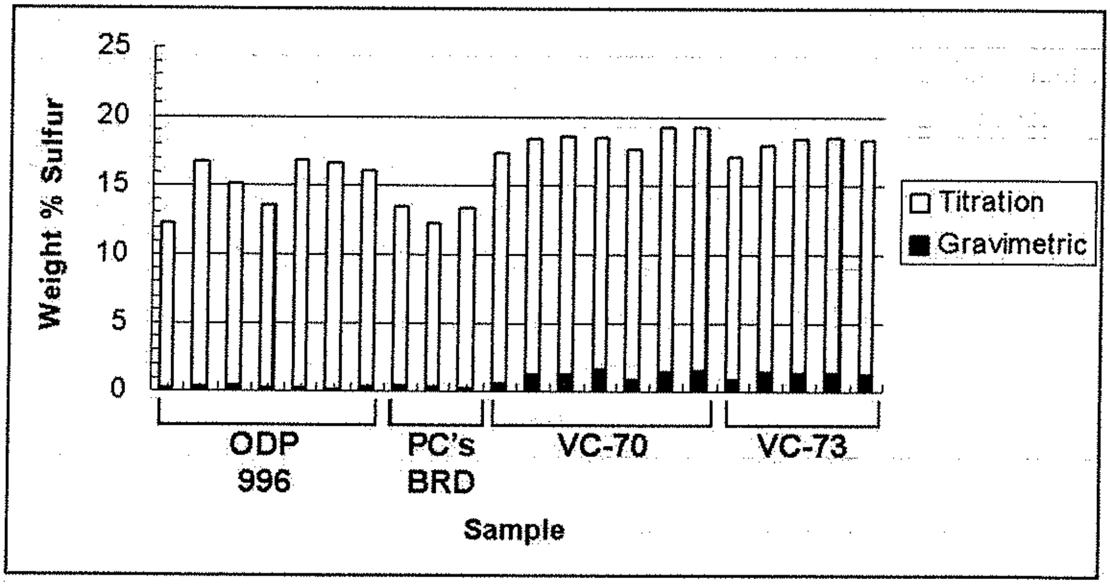

Figure 5. Sulfide sulfur concentration of seep-site sediments. Note the varying values for two different measurement methods: iodometric titration vs. gravimetric analysis.

And Kaplan, 1979; Sweeney and Kaplan, 1980). Sulfide sulfur concentrations from the gravimetric analysis are more consistent with these other findings, typically showing less than 2% sulfur (Fig. 6). In contrast, iodometric analyses yield sulfide sulfur concentration of 12–18 weight percent sulfur (Fig. 7). Monterey Bay seep sites (Kohn et al., 1998) have yielded sulfide sulfur values of ~2–4%, making our titration values suspect. Our gravimetric analysis yielded values of sulfide sulfur for Monterey Canyon from 1-2%, and therefore are lower than those found by Kohn et al. (1998). Even though our gravimetric results are perhaps incorrect, they will be used for comparisons with sulfur geochemistry from diffusive sites.

Our laboratory results are unreliable as evidenced by low recoveries of sulfur from pyrite standards. Possible reasons for this lowered recovery are: 1. Insufficient concentration of the trapping solution to precipitate potentially greater amounts of sulfur in seep site sediments. 2. Bubbling too quickly in the trapping flask, which would increase the probability that sulfide gas would escape without precipitating. 3. Loss of sulfide gas from the reaction flask while adding the chromic chloride solution. 4. Leakage of sulfide gas from the extraction apparatus. 5. Incorrect chemical balance created by increasing the concentration of KI/KIO_3 solution without increasing concentration of ammonium hydroxide in the trapping solution.

Sulfide sulfur content for both iodometric titration and gravimetric methods for each specific site are tabulated in Table 2 (Appendix B) and shown in Figures 6 and 7. In all cases sulfur sulfide content is higher in iodometric analysis but these data are likely flawed as discussed above. The data from the gravimetric method may or may not be valid so we will not discuss the data of specific sites.

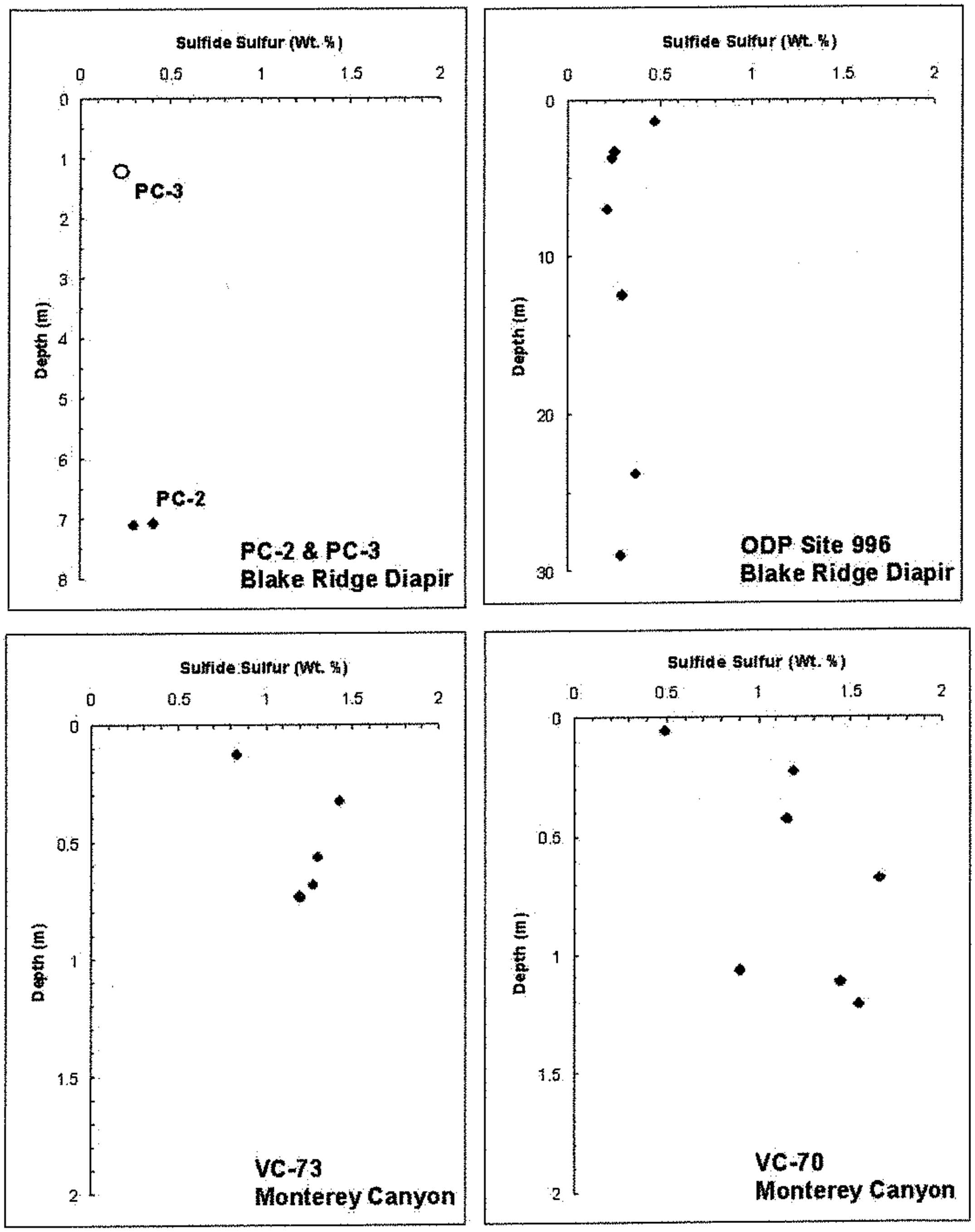

Figure 6. Depth profiles of sulfide sulfur concentration (Wt %) determined by gravimetric means using silver sulfide precipitate. Seep samples at the Blake Ridge Diapir include those from both piston cores (PC-2, PC-3) and drill cores (Ocean Drilling Program Site 996). Seep samples at the Monterey Canyon were taken by vibracoring at two sites VC-73 and VC-70.

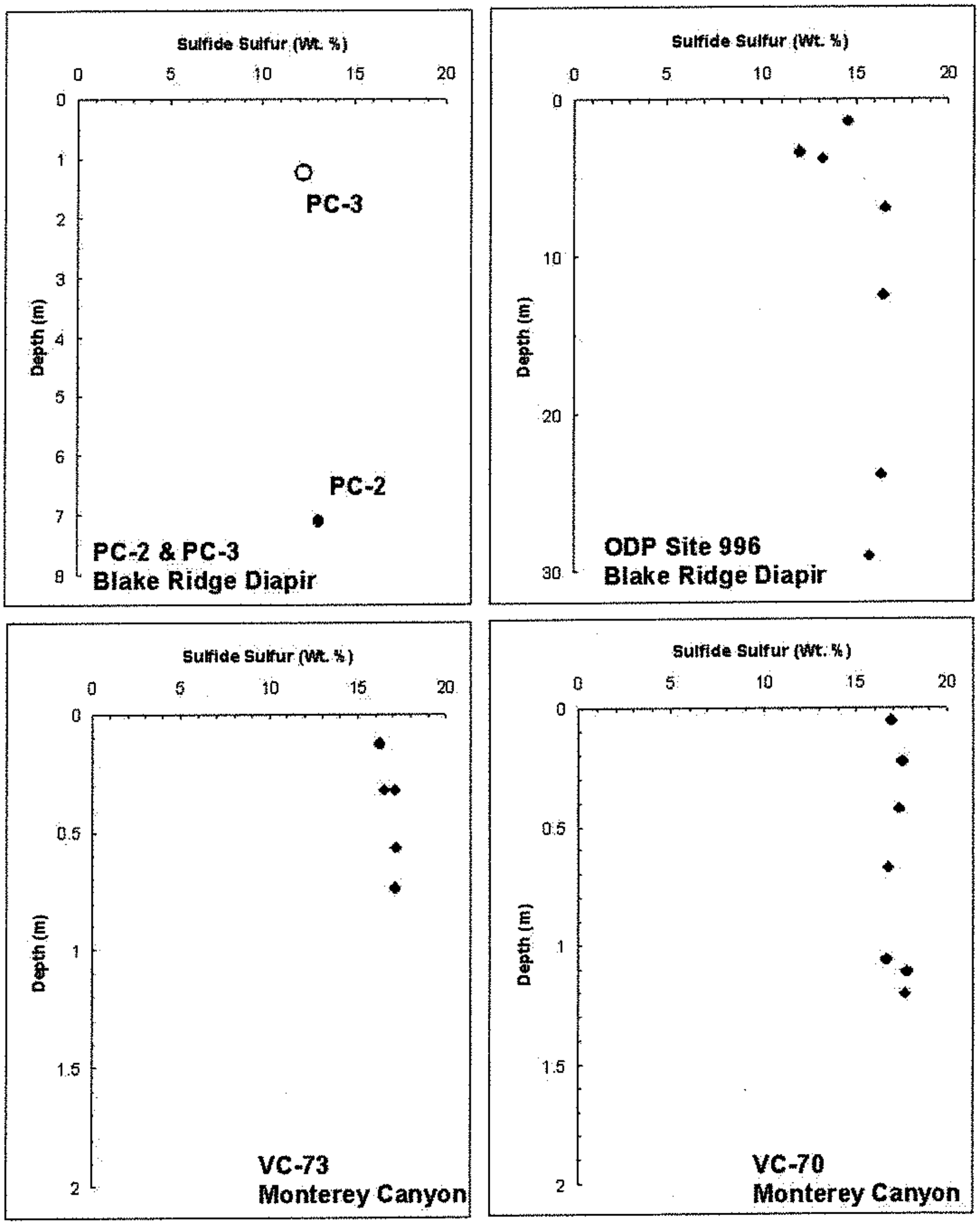

Figure 7. Depth profiles of sulfide sulfur concentration (Wt %) determined by iodometric titration using zinc sulfide precipitate. Seep samples at the Blake Ridge Diapir include those from both piston cores (PC-2, PC-3) and drill cores (Ocean Drilling Program Site 996). Seep samples at the Monterey Canyon were taken by vibracoring at two sites VC-73 and VC-70.

Results are pending from the results of the isotopic concentration from this study; however, literature reviews will supply data concerning isotopic composition of seep sites in Monterey Canyon (Kohn et al. 1998).

Literature Results

We compare the sulfide sulfur content (Fig. 8) and sulfur isotopic composition (Fig. 9) of seep sites versus diffusive sites using data from the literature. We use previous studies of both the Blake Ridge region and Monterey Canyon seep sites. Diffusive sites of the Blake Ridge region were studied by Borowski et al. (2000b; in prep), Takacs and Borowski (2003, 2004), and Thompson and Borowski (2004). The sulfur biogeochemistry of Monterey Canyon seep sites has been studied by Kohn et al. (1998).

Figure 8 compares the amount of sulfide sulfur in sediments at seep sites (this study) and diffusive sites of the Blake Ridge region. For both comparisons, the data from diffusive sites have been differentiated into depth zones that have been affected by different biogeochemical processes. Sediments from the sediment-water interface to a depth of 1 meter above the sulfate-methane interface have likely only experienced sulfate reduction through oxidation of sedimentary organic matter. The sediment from 1 meter above the SMI and below has been affected by the additional, sulfate-reduction process of anaerobic methane oxidation.

Sulfide content among the three sediment categories overlap, however, there are differences between the categories. There is a general increase in sulfur content from sediments affected by SOM to those affected by AMO to those at seep sites. Sediments from diffusive sites affected by AMO tend to have higher amounts of sulfide sulfur than those exclusively affected by SOM. Seep sites show two distinct populations with Blake Ridge sediments having significantly less sulfur than Monterey Bay seep sediments with one exception (VC-70, 4–7 cm, Monterey Bay). Because of this distribution the Blake Ridge seep sediments cannot be distinguished from diffusive site sediments, whereas, the

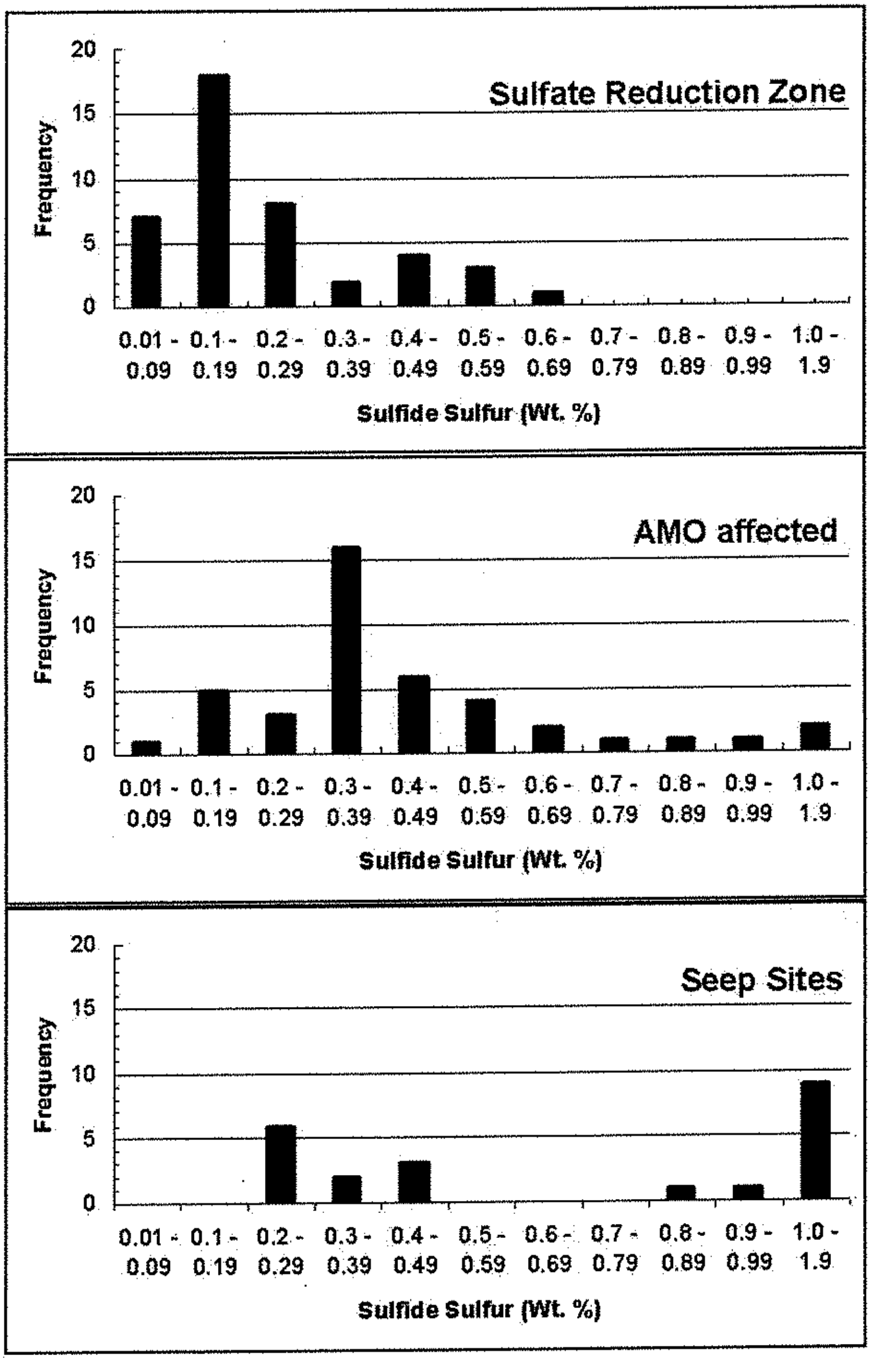

Figure 8. Comparison of sulfide sulfur concentration (Wt. %) at seep sites and diffusive sites of the Blake Ridge. Seep data are from both Blake Ridge Diapir and Monterey Canyon. Other data were generated by Borowski et al. (in prep.), by Takacs (2003, 2004), and by Thompson et al. (2004). Samples from the sulfate reduction zone of diffusive sites occur between the sediment-water interface and to within 1 m of the sulfate-methane interface (SMI). Samples potentially affected by AMO occur from 1 m above the SMI, thru the SMI, and into the present methanogenic zone below. Note that seep sites generally contain more authigenic sulfide sulfur.

Monterey Canyon seep sediments overlap in sulfide content with sediments from diffusive sediments affected by AMO. Therefore it cannot be determined if a site is diffusive or advective based on the sulfide content of the sediments alone. Perhaps seep sediments can be determined by their sulfur isotopic composition.

Figure 9 compares the sulfur isotopic compositions ($\delta^{34}S$) of seep-site sediments from Monterey Canyon as found by Kohn et al. (1998), and sediments from diffusive sites of the Blake Ridge region. We use the same three categories as above. Modes for each sediment category show slight differences with seep sites showing an intermediate peak between each category of diffusive sites. Sediment affected by only SOM tends to be enriched in ^{32}S relative to sediments affected by AMO. Despite these modal differences, isotopic values from seep sites overlap with both diffusive site categories and therefore cannot be distinguished isotopically. Only one sediment type has a unique isotopic composition: a number of samples from AMO-affected sediments from diffusive sites are more enriched in ^{34}S, showing positive $\delta^{34}S$ values.

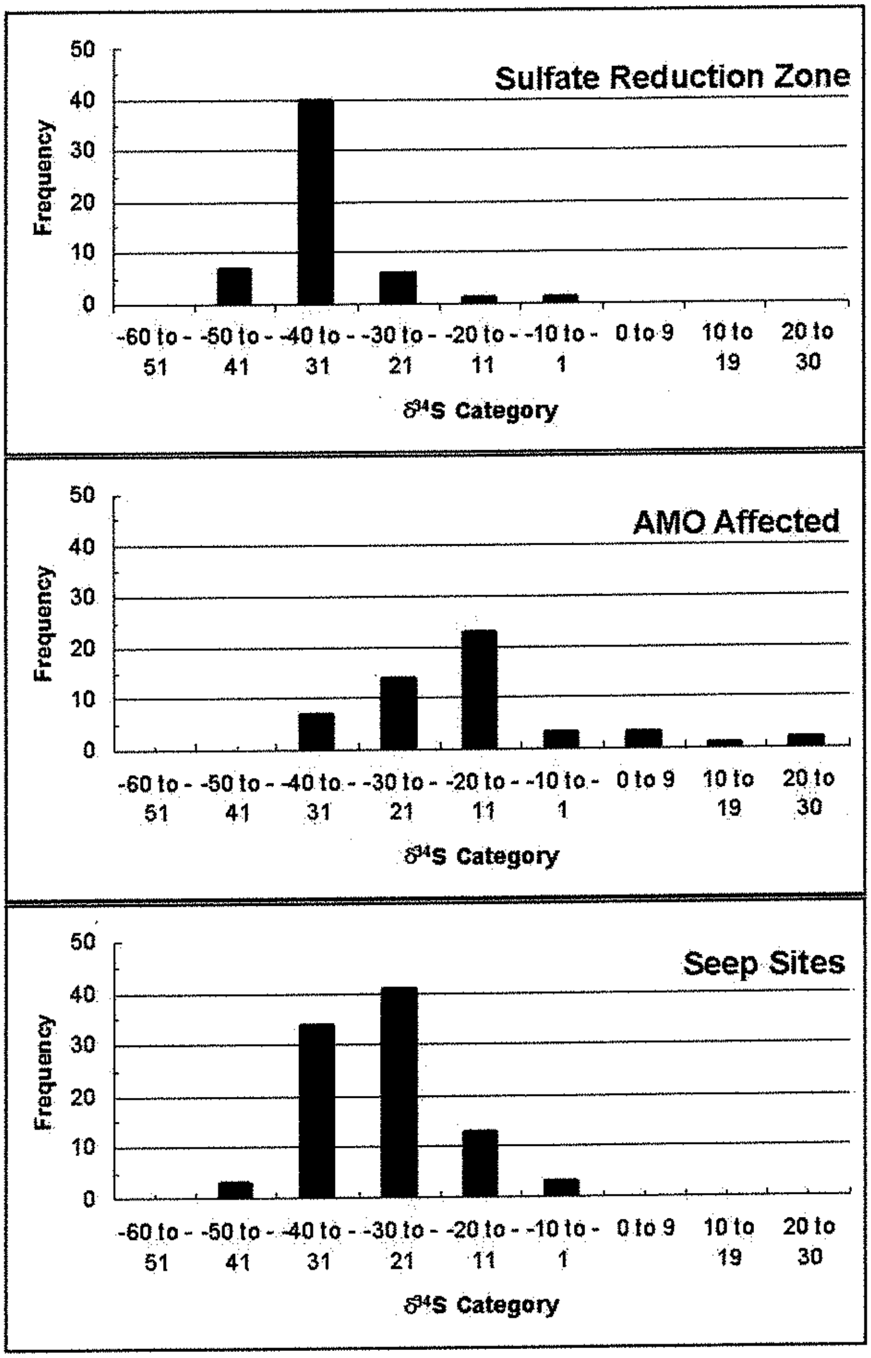
Sulfate Reduction Zone

AMO Affected

Seep Sites

Figure 9. Comparison of sulfur isotopic composition ($\delta^{34}S$) of authigenic sulfide minerals at seep sites of Monterey Bay, and diffusive sites of the Blake Ridge region. Seep data are from both Blake Ridge Diapir and Monterey Canyon. Other data were generated by Borowski et al. (in prep.), by Takacs and Borowski (2003, 2004), and by Thompson et al. (2004). Sediments potentially affected by AMO seem to be enriched in ^{34}S.

Discussion

The sulfur geochemistry of marine sediments is influenced by a myriad of complex, biogeochemical processes (e.g., Chambers and Trudinger, 1978; Berner, 1980; Jourgensen, 1990). Sulfur disproportionation and both pathways of sulfate reduction occur in most disoxic and anoxic sediments. SOM is an important process in early diagenesis that reduces sulfate to sulfide. Sulfur disproportionation involves the creation of both dissolved sulfate and sulfide from solid-phase, elemental sulfur usually formed by SOM, and is responsible for extreme ^{32}S enrichment in sulfide-sulfur minerals (Canfield and Thamdrup, 1994). Anaerobic methane oxidation is an additional process that affects sulfur geochemistry. Moreover, sulfur geochemistry is likely influenced by mass transport processes of both sulfate and methane.

AMO occurs at both diffusive and advective sites, but AMO reaction rates are likely higher at advective sites because of increased methane and sulfate delivery rates. With increased AMO rates its geochemical effects likely become more significant and recognizable. The production of more dissolved sulfide in pore waters via AMO should result in the formation of more authigenic sulfide minerals, increasing the sulfide-sulfur content of the sediments at seep sites. AMO may also influence the sulfur isotopic composition of sulfide sulfur in marine sediments.

Sulfide Sulfur Content

Our sulfide sulfur concentration data are unreliable because: 1. Low recovery rate of sulfide sulfur from pyrite standard throughout this study. 2. Lack of pyrite standards for some extraction runs. 3. Extreme disagreement between iodometric titration and gravimetric methods. 4. Disagreement with published values from the same general area. Therefore, any discussion of these data here would be groundless.

Sulfur Isotopic Composition

The isotopic composition of sulfide sulfur in authigenic sulfide minerals from diffusive and advective sites may provide clues to their biogeochemical processes.

Diffusive Sites

Diffusive sites of the Blake Ridge region are influenced by AMO (Borowski et al., 1996, 1997, 2000a), and this influence is evident in the sulfur geochemistry. Sulfate depletion occurs throughout the SRZ, and as sulfate is used by sulfate-reducing bacteria ^{32}S is preferentially depleted leaving a sulfate pool enriched in ^{34}S (Fig. 1). Because of fractionation involved in sulfate reduction, the dissolved sulfide pool also becomes more enriched in ^{34}S with depth into the SRZ. The isotopic composition of the solid phase sulfide nearly mirrors that of the dissolved sulfide pool because there is about $1^{\circ}/_{\circ\circ}$ fractionation involved in precipitation (Price and Shieh, 1979; Wilkin and Barnes,1996). The amount of sulfide minerals in sediments tend to gradually increase with depth in the SRZ, but also show larger amounts below the present-day SMI (Fig. 1). There is also a similar trend toward ^{34}S enrichment with depth in the SRZ that often peaks near the SMI, and similar enrichments also occur below the present-day SMI (Fig. 1).

Borowski et al., (in prep) argue that sulfur disproportionation, SOM, and AMO create characteristic isotopic signatures within Blake Ridge sediments (Fig. 10). In the uppermost sulfate reduction zone, sulfide minerals are precipitated and sulfur

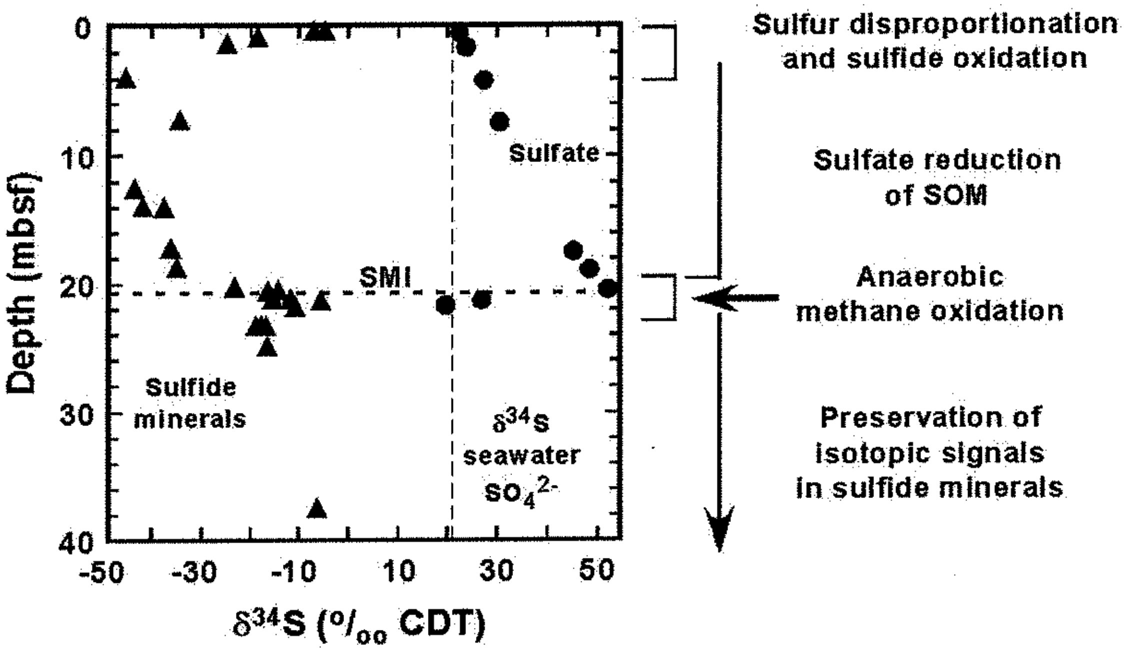

Figure 10. Depth zonation of biogeochemical process that influence sulfur geochemistry. The depth profile shows the sulfur isotopic composition ($\delta^{34}S$) of pore-water sulfate and authigenic sulfide minerals in sediments of Ocean Drilling Program (ODP) Site 995. Diffusion of dissolved substances is the dominant form of mass transport at Site 995. After Borowski et al. (in prep.).

disproportionation drives the sulfur isotopic composition of the minerals to extreme ^{34}S depletion ranging from -40 to -50‰ (Canfield and Thamdrup, 1994). These very negative $\delta^{34}S$ values create a baseline because any subsequent addition of sulfide minerals deeper in the SRZ will be more enriched in ^{34}S due to the evolution of the dissolved sulfate and sulfide pools toward increasing ^{34}S with depth as SOM occurs. Near the SMI, anaerobic methane oxidation becomes an important process causing dissolved sulfide production and authigenic sulfide mineral formation at a specific depth zone. Because dissolved sulfate and sulfide are maximally enriched in ^{34}S near the SMI, sulfide minerals formed there will also be enriched in ^{34}S. Below the SMI these isotopic signals should be preserved in the sedimentary record.

Advective Sites

The sulfur isotopic composition of sulfide minerals at seep sites from the Blake Ridge region and Monterey Bay are intermediate in modal $\delta^{34}S$ values between sulfide minerals formed in the SRZ and those near the SMI. Therefore, authigenic sulfide minerals formed in seep sediments cannot be distinguished isotopically from those of diffusive sites (Fig 9). Also, more extreme ^{34}S enrichment via AMO occurs under diffusive conditions. We suspect that the sulfate pool at seep sites experiences less ^{34}S enrichment because of increased sulfate delivery rate from overlying seawater with constant sulfur isotopic composition ($\delta^{34}S$=21‰ CDT; Rees et al., 1978).

When advection occurs, methane is carried through the sediment and is delivered at a faster rate than through diffusion alone. As a result, the sulfate reduction zone shrinks to centimeters to meters in thickness as AMO rates are stimulated. The sulfate-methane interface moves closer to the sediment-water interface and reaches equilibrium with downward sulfate delivery by diffusion (Borowski et al., 1996). The pathway of sulfate diffusion is thus shortened so that less fractionation of sulfate sulfur occurs within the sediments, moving the sulfur isotopic composition of dissolved sulfide and sulfide minerals to more negative $\delta^{34}S$ values. Under diffusive conditions, sulfide sulfur derived from pore-water sulfate showing $\delta^{34}S$ values of -50 $^{o}/_{oo}$ near the SMI (e.g., Fig.1) then shows more enrichment in ^{34}S with positive $\delta^{34}S$ values in the mineral phase (Figs. 1 and 9).

Implications

The sulfur isotopic composition of authigenic sulfide minerals within sediments formed in association with AMO under diffusive conditions is apparently unique in today's oceans, being significantly more enriched in ^{34}S. These sediments can be distinguished from those at methane seeps, and from sediments affected by SOM under diffusive conditions. Because sulfur isotopic signals should be preserved within the sediment and rock record, discrete enrichments of ^{34}S in sulfide minerals may identify the stratigraphic location of sulfate-methane occurring in the geologic past. This knowledge may allow further insight concerning the oxidation of the world's oceans in the Precambrian (Borowski, personal communication).

SUMMARY

(1) Our sulfide sulfur concentration measurements are likely incorrect.

(2) Seep site sediments from Monterey Bay seem to have higher amounts of sulfide sulfur residing in authigenic sulfide minerals than those from the Blake Ridge Diapir.

(3) Seep site sediments cannot be distinguished from diffusive site sediments based on the amount of sulfide sulfur.

(4) Seep site sediments cannot be distinguished from diffusive site sediments based on the sulfur isotopic composition of authigenic sulfide minerals.

(5) Sediment samples from near the sulfate-methane interface (likely affected by AMO) of diffusive sites in the Blake Ridge region have a unique isotopic signature more enriched in ^{34}S.

References

Berner, R.A., 1980. Early Diagenesis, A Theoretical Approach. Princeton University Press, Princeton.

Borowski, W.S., Paull, C.K., 1996. Marine pore-water sulfate profiles indicate in situ methane flux from underlying gas hydrate. *Geology*, v. 24, no. 7, 655-658.

Borowski, W. S., Paull, C.K., Ussler III, W., 1997. Carbon cycling within the upper methanogenic zone of continental-rise sediments: An example from the methane-rich sediments overlying the Blake Ridge gas hydrate deposits. *Marine Chemistry*, v. 57, 299-311.

Borowski, W.S., 1998. Pore Water Sulfate Concentration Gradients, Isotopic Compositions, and Diagenetic Processes Overlying Continental Margin, Methane-Rich sediments associated with Gas Hydrates. Ph.D. Dissertation, University of North Carolina, Chapel Hill, North Carolina, USA.

Borowski, W.S., Paull, C.K., Ussler III, W., 1999. Global and local variations of interstitial sulfate gradients in deep-water, continental margin sediments: Sensitivity to underlying methane and gas hydrates. *Marine Geology*, v. 159, 131-154.

Borowski, W.S., Hoehler, T.M., Alperin, M.J., Rodriguez, N.M., Paull, C.K., 2000a. Significance of anaerobic methane oxidation in methane-rich sediments overlying the Blake Ridge gas hydrates. In: Paull, R. Matsumoto, Wallace, P.J., Dillon, W.P. (Eds.), Gas Hydrate Sampling on the Blake Ridge and Carolina Rise. *Proceedings ODP, Scientific Results*, 164, College Station, TX, pp. 87-99.

Borowski, W.S., Paull, C.K., Ussler III, W., 2000b. Isotopic composition of authigenic sulfide minerals at the base of the sulfate-reduction zone: Implications for diagenesis at the sulfate-methane interface. *EOS Transactions American Geophysical Union (AGU)*.

Borowski, W.S., C.K. Paull, And William Ussler III. 2002. The meeting of two microbial worlds: Geochemistry of the sulfate-methane interface. http://joiscience.org:16080/greatesthits2/pdfs/borowski.pdf.

Borowski, W.S., Rodriguez, N.M., Paull, C.K., Ussler III, W. In preparation, 2003. Significance of ^{34}S-enrichments in authigenic sulfide minerals: Implications for earth history.

Canfield, D.E., Raiswell, R., Westrich, J., Reaves, C., Berner, R.A., 1986. The use of chromium reduction in the analysis of reduced inorganic sulfur in sediments and shales. *Chemical Geology*, v. 54, 149-155.

Canfield, D.E., Thamdrup, B., 1994. The production of ^{34}S-depleted sulfide during bacterial disproportination of elemental sulfur. *Science*, v. 266, 1973-1975.

Chambers, L.A., Trudinger, P.A., 1978. Microbiological fractionation of stable sulfur isotopes: A review and critique. *Geomicrobiology J.*, v. 1, 249-293.

Egeberg, P.K., 2000. Hydrates Associated With Fluid Flow Above Salt Diapirs (Site 996). In: Paull, R. Matsumoto, Wallace, P.J., Dillon, W.P. (Eds.), Gas Hydrate Sampling on the Blake Ridge and Carolina Rise. *Proceedings ODP, Scientific Results*, 164, College Station, TX, 219-228.

Embley, R.W., Eittreim, S.L., McHugh, C., Normark, W.R., Rau, G.H., Hecker, B., DeBevoise, A.E., Greene, H.G., Ryan, W.B.F., Harrold, C., and Baxter, C., 1990, Geological setting of chemosynthetic communities in the Monterey Fan Valley system: Deep-Sea Research, v. 37, 11, 1651-1667.

Goldhaber, M.B., Kaplan, I.R., 1979. Mechanisms of sulfur incorporation and isotope fractionation during early diagenesis in sediments of the Gulf of California. *Marine Chemistry*, 9, 95-143.

Holt, B.D., Engelkemeir, A.G., 1970. Thermal decomposition of barium sulfate to sulfur dioxide for mass spectrometric analysis. *Analytical Chemistry*, v. 42, 1451-1453.

Jorgensen, B.B., 1983. The microbial sulfur cycle. In: Krumbein, W.E. (Ed.), Microbial Geochemistry, St. Louis, Blackwell Scientific Publications, pp. 91-124.

Kendall, C., Snider, D., 1995. Resources on isotopes. www.rcamnl.wr.usgs.gov/isoig/period/s_iig.html USGS 2004.

Kohn, M.J., Riciputi, L.R., Stakes, D., Organge, D.L., 1998. Sulfur isotope variability in biogenic pyrite: Reflections of heterogeneous bacterial colonization? *American Mineralogist*, v. 83, 1454-1468.

Orphan, V.J., House, C.H., Hinrichs, K., McKeegan, K.D., DeLong, E.F., 2001. Methane-consuming Archaea revealed by directly coupled isotopic and phylogenetic analysis. *Science*, v. 293, 484-487.

Paull, C.K., Ussler, W. III, Borowski, W.S., Speiss, F.N., 1995. Methane-rich plumes on the Carolina continental rise: Associations with gas hydrates. *Geology*, v. 23, 89-92.

Paull, C.K., Matsumoto, R., Wallace, P.J., et al., 1996. *Proceedings ODP, Initial Reports*, 164, College Station, Texas, Ocean Drilling Program.

Price, F.T., Shieh, Y.N., 1979. Fractionation of sulfur isotopes during laboratory synthesis of pyrite at low temperatures. *Chemical Geology*, v. 27, 245-253.

Rees, C. E., Jenkins, W. J., Monster, J., 1978. The sulphur isotopic composition of ocean water sulphate. *Geochimica Cosmochimica Acta*, v. 42, 377-381.

Sweeney, R.E., Kaplan, I.R., 1980. Diagenetic sulfate reduction in marine sediments. *Marine Chemistry*, v. 9: 165-174.

Takacs, K.G., Borowski, W.S., 2003. Authigenic sulfide mineralization induced by anaerobic methane oxidation in methane-rich, gas-hydrate-associated sediments: Stratigraphic patterns of sulfide sulfur concentration and sulfide-sulfur isotopic composition. *GSA Abstracts Programs*, v. 35, no. 1, 4.

Takacs, K.G., Borowski, W.S., 2004. Changes in sulfur concentration and sulfur isotopic composition within authigenic sulfide minerals from sediments of Miocene age to the present, ODP Site 995, Blake Ridge, offshore southeastern United States. *GSA Abstracts Programs*, v. 36, no.2, 47.

Thompson, M.K., Borowski, W.S., 2003. Sulfide mineralization in deep-water marine sediments related to methane transport, methane consumption, and methane gas hydrates. *J. Kentucky Academy Science*.

Thompson, M.K., Borowski, W.S., Ussler, W. III, Paull, C.K., 2004. Sulfide mineralization in deep-water marine sediments related to methane transport, methane consumption, and methane gas hydrates. *GSA Abstracts Programs*, 36(2), 124.

Wilkin, R.T., Barnes, H.L., 1996. Pyrite formation by reactions of iron monosulfides with dissolved inorganic and organic sulfur species. *Geochimica Cosmochimica Acta*, v. 60, 4167-4179.

APPENDIX A

Table 1. List of samples used for this study. Sediment samples for this study were sampled from both Monterey Canyon and Blake Ridge Diapir methane seep sites.

Monterey Canyon	**Blake Ridge Diapir**
VC-70, 4 -7 cm	996B, 1H-02, 52-67 cm
VC-70, 20-25 cm	996D, 4H-2, 10-25 cm
VC-70, 40-45 cm	996E, 1H-1, 135-150 cm
VC-70, 65-70 cm	996E, 1H-3, 72-87 cm
VC-70, 104-109 cm	996E, 2H-2, 135-150 cm
VC-70, 109-114 cm	996E, 2H-6, 117-132 cm
VC-70, bottom 15 cm	996E, 4H-5, 135-150 cm
VC-73, 10-15 cm	PC-3, 118-124 cm
VC-73, 30-35 cm	PC-2, 705-711 cm
VC-73, 54-59 cm	PC-2, bottom 15 cm
VC-73, 66-71 cm	
VC-73, 71-76 cm	

APPENDIX B

Table 2. Sulfide-sulfur concentration in weight percent sulfur (Wt. % Sulfur) expressed in authigenic sulfide minerals of the methane seep sites of the Blake Ridge Diapir and Monterey Bay.

Location	**Sample**	**Titration (Wt. % Sulfur)**	**Gravimetric (Wt. % Sulfur)**
Blake Ridge Diapir	996B, 1H-2 52-67 cm	12.0	0.26
	996D, 4H-2 10-25 cm	16.4	0.38
	996E, 1H-1 135-150 cm	14.6	0.48
	996E, 1H-3 72-87 cm	13.3	0.24
	996E, 2H-2 135-15 cm	16.6	0.22
	996E, 2H-6 117-132 cm	16.5	0.30
	996E, 4H-5 135-150 cm	15.8	0.29
	PC-2, 705-711 cm	13.1	0.41
	PC-2, bottom 15 cm	12.0	0.31
	PC-3, 118-124 cm	13.1	0.24
Monterey Canyon	VC-70, 4-7 cm	16.9	0.49
	VC-70, 20-25 cm	17.5	1.19
	VC-70, 40-45 cm	17.4	1.16
	VC-70, 65-70 cm	16.8	1.66
	VC-70, 104-109 cm	16.7	0.91
	VC-70, 109-114 cm	17.8	1.45
	VC-70, bottom 15 cm	17.7	1.55
	VC-73, 10-15 cm	16.3	0.83
	VC-73, 30-35 cm	16.5	1.43
	VC-73, 54-59 cm	17.1	1.30
	VC-73, 66-71 cm	17.2	1.28
	VC-73, 71-76 cm	17.1	1.20